



On-line monitoring of key nutrients in yoghurt samples using digitally labelled Raman spectroscopy

Da Chen ^{a,b}, Yang Li ^a, Zong Tan ^a, Zhi-xuan Huang ^a, Jing Zong ^a, Qi-feng Li ^{a,*}

^a College of Precision Instrument and Opto-Electronics Engineering, Tianjin University, Tianjin 300072, China

^b Centre for Aircraft Fire and Emergency, Civil Aviation University of China, Tianjin, 300300, China

ARTICLE INFO

Article history:

Received 15 May 2018

Received in revised form

8 April 2019

Accepted 8 April 2019

Available online 29 April 2019

ABSTRACT

On-line monitoring of the fermentation process is essential for improving the quality of yoghurt products. We developed an on-line monitoring system based on digitally labelled Raman spectroscopy (DLRS). In DLRS, the strategy of Monte Carlo competitive adaptive reweighted sampling selection was proposed to isolate spectral bands according to a high-density discrete wavelet transform domain, which greatly suppressed the matrix effect on the calibration models. We demonstrated the feasibility of DLRS using 72 practical samples, and 4 key nutrients protein, fat, sucrose and total solids were determined simultaneously. The satisfactory results indicate that the DLRS system has capability for on-line monitoring of 4 key nutrients during yoghurt fermentation, thus enabling intelligent control of yoghurt production.

© 2019 Elsevier Ltd. All rights reserved.

1. Introduction

Yoghurt represents one of the most completely nutritious foods that is consumed throughout much of the world (Lopez-Garcia, Leon-Munoz, Guallar-Castillon, & Rodriguez-Artalejo, 2015; Williams, Hooper, Spiro, & Stanner, 2015). The nutrient content of yoghurt samples before fermentation greatly affects the quality of the final product, in which four ingredients protein, fat, sucrose and total solids are extremely important. In yoghurt production, protein is an important criterion for dairy nutrition (Ipsen, 2017), while fat affects not only nutrition but also flavour of yoghurt products (Pereira, Singh, Munro, & Luckman, 2003). Sucrose represents a source of carbohydrates to increase the water holding capacity and viscosity of yoghurt products, which improves the flavour. Total solids affects the gelation of proteins during yoghurt fermentation, which determines the solidification state of yoghurt (Rodriguez et al., 2013; Singh & Muthukumarappan, 2008; Torres, Janhøj, Mikkelsen, & Ipsen, 2011). This creates a demand to determine the amount of these four components to optimise the production process.

Analytical approaches for determination of the four components mainly rely on off-line analytical techniques, such as Kjeldahl determination (Jones, 1991), Soxhlet extraction, and high pressure liquid chromatography (Castiglioni, Bagnati, Calamari, Fanelli, &

Zuccato, 2005). These off-line methods require complicated wet chemical steps of extraction, digestion, separation as well as laborious work, which is not capable of optimising yoghurt fermentation process in a timely manner. An on-line monitoring approach is thus required for further enhance quality control of yoghurt products (Williams et al., 2015).

Several methods have been proposed for on-line monitoring (Fitzgerald, McGrath, O'Connor, & Phelan, 1998), with the majority of these methods focussing on the methods of near infrared spectroscopy (NIR) (Brennan, Alderman, Sattler, O'Connor, & O'Mathuna, 2003) and infrared spectroscopy (IR) (Karoui, Mazerolles, & Dufour, 2003; Wojciechowski, Melilli, & Barbano, 2016). However, the high water content in yoghurt samples and shallow illumination depth combine to limit the application of NIR and IR spectroscopy for on-line monitoring of yoghurt samples, thus a water-resistant and large illumination depth method for on-line measurement of yoghurt products is required.

Raman spectroscopy provides a potential solution to this challenge, presenting unique advantages for on-line measurement of solution systems with relatively large illumination depth (Luo et al., 2016; Wang et al., 2017). Raman spectroscopy is capable of illuminating the yoghurt samples through windows on the pipe, and the Raman spectral bands of water are weak (Nieuwoudt, Holroyd, McGovern, Simpson, & Williams, 2016). However, the highly overlapped spectral bands and uncontrolled matrix effect combine to spoil Raman spectral analysis, which requires a sophisticated chemometrics method for assigning Raman spectral bands to

* Corresponding author. Tel.: +86 22 27404209.

E-mail address: qfli@tju.edu.cn (Q.-f. Li).

components of interest (Doganis & Sarimveis, 2007; Tsarouhas & Arvanitoyannis, 2014).

Raman spectra are inherently multiscaled in nature, containing spectral bands localised differently in both time (wavelength position) and frequency (peak width position) domains (Feudale, Liu, Woody, Tan, & Brown, 2005; Han et al., 2017c; Woody & Brown, 2010). It is thus expected that higher-density discrete wavelet transform (HDWT) with multi-resolution capability may isolate the Raman spectral bands related to analytes well (Han et al., 2017b,c; Liu & Brown, 2004). The oversampling strategy in HDWT enhances the time–frequency plane with a density that is three times higher than that of routine wavelet transform (Tan et al., 2017). This would provide valuable expansion capability to discriminate the bands of key ingredients from overlapped spectra of yoghurt matrix. With the combination of feature selection methods, important HDWT coefficients related to the spectral bands of key nutrients could be selected accurately.

Several feature selection procedures have been developed to extract important variables related to analytes of interest, including uninformative variable elimination (UVE) (Roupas, 2008), modified iterative predictor weighting (mlPW) (Chen, Cai, & Shao, 2007), competitive adaptive reweighted sampling selection (CARSS) (Li, Liang, Xu, & Cao, 2009) and its derivation, randomisation tests (Gomez-Carracedo, Andrade, Rutledge, & Faber, 2007). Of these, CARSS provides the unique advantage of constructing a parsimonious model with a very small number of reasonable predictors (Li et al., 2009). However, the CARSS results varied from run to run because of its random resampling procedure. To improve the stability of the CARSS calculation, a Monte Carlo resampling strategy is proposed in this work, i.e., Monte Carlo CARSS (MCCARSS). MCCARSS collects all the feature selection results obtained by multiple runs of CARSS, and then counts the frequency of each variable presented in the MCCARSS matrix. With the criterion of minimum prediction error, variables with the highest frequencies were selected for future multivariate calibration.

The present study introduces the strategy of digitally labelled Raman spectroscopy (DLRS) for on-line monitoring of key ingredients in homogenised yoghurt samples before pasteurisation. The DLRS system combines an on-line Raman instrument and a systematic chemometrics method that consists of HDWT and MCCARSS, which does not need any chemical analysis. The cost of the DLRS system is also reasonable for dairy industry when compared with the correspondingly routine analytical instruments, thus providing a promising tool for real time monitoring of key ingredients in yoghurt samples.

2. Materials and methods

2.1. Sample preparation

In the yoghurt production process used here, refrigerated raw milk was heated to 55 °C to dissolve sucrose and other stabilisers efficiently. After 30–60 min of mixing, the homogenised yoghurt samples were gradually dropped to a lower temperature, such as 5 °C, for further pasteurisation. What should be stressed here is that 25 °C is an intermediate temperature during the cooling process, which is used as a sampling temperature for off-line measurement of ingredient contents in yoghurt samples.

In this work, 72 homogenised yoghurt samples before pasteurisation were collected from 8 batches (9 samples each week). Samples were sealed and packed in 1 L sampling bottles, and refrigerated at 0–2 °C. Before the Raman spectra collection, the yoghurt samples were heated in a water bath to 25 °C, which simulates the temperature of the practical yoghurt sampling. Ten spectra of each yoghurt sample were recorded for average, each with 5 s exposure time. Samples were randomly divided into two parts, one part with 48 samples was used as the training set, and the remaining 24 samples was used as the validation set.

2.2. Designing of the experimental system

2.2.1. Raman spectrometer

Raman spectra were recorded using a MilkEye2000 Raman system (SmartData Tech Co., Ltd. Tianjin, China) with a back scattering probe (Han et al., 2017a,c). The instrument uses a 785 nm single-mode diode laser source with a max power of 100 mW. Back scattered light was collected using a free space design, and a volume-phase holographic grating disperses the light over an image plane measured in the charge coupled device (CCD) with 1024 × 64 pixels, spanning a Raman shift interval from 200 to 2200 cm^{-1} . Here, the pixel size of the CCD is 14 μm × 14 μm , capturing a wavenumber interval around 3 cm^{-1} . The signal-to-noise ratio of the Raman spectrometer is 500:1. In the Raman spectral measurement, integration time was set to 5s, while the power of laser and CCD temperature were set as 90 mW and 14 °C, respectively.

2.2.2. On-line monitoring pipeline

In the practical yoghurt production process, the temperature of the homogenising pipeline of yoghurt samples before pasteurisation varies from 0 °C to 65 °C, accompanied with strong vibration.

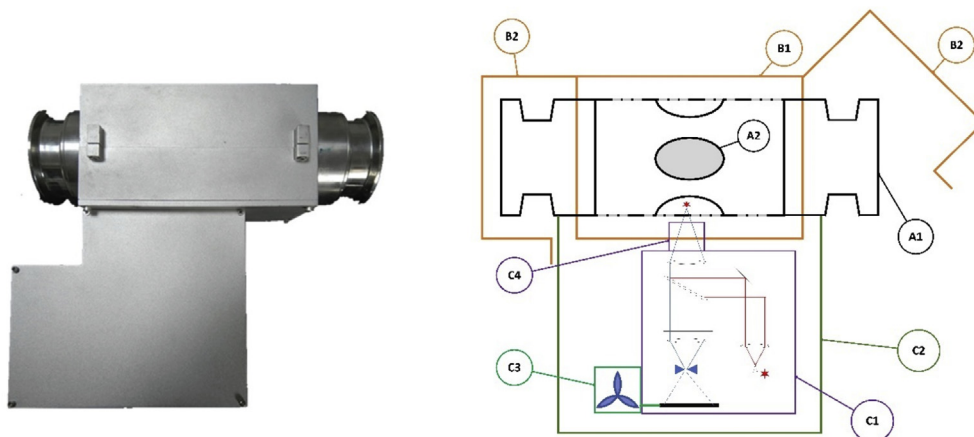


Fig. 1. Structure diagram of the on-line Raman system: A1, stainless steel body; A2, Teflon window; B1, B2, airtight covers; C1–C4, separate shielded enclosure with an active heat sink.

This required a sophisticated Raman system to adapt the complex production environment of yoghurt products (Fig. 1). Here, we chose a horizontal part of the homogenising pipeline to simulate practical on-line measurement, which consists of stainless steel body and a Teflon window. This pipeline had an outer diameter of 8.9 cm, an inner diameter of 6.9 cm, a length of 30.4 cm, and the translucent window with a thickness of 0.4 cm.

To the above on-line pipe design, the Raman spectrometer was fixed to the pipeline with moving locks, making it easy to disassemble or reload samples. An airtight cover with a rubber ring can not only overcome the pipe vibration, but also avoid the interference of external light. What should be stressed is that the airtight covers at both ends are only used in the simulation experiments, and effects of flow on the on-line measurement results should be further evaluated in practical applications. The Raman spectroscopy system was installed in a separate shielded enclosure with an active heat sink, which maintains the CCD temperature of Raman spectrometer.

2.3. Data analysis of on-line Raman spectra

The on-line Raman spectra were affected by not only the Teflon window but also the matrix of yoghurt samples, resulting in distorted Raman signals. The spectral bands of key ingredients need to be isolated from the raw Raman spectra before multivariate calibration. In this regard, HDWT was adopted to provide an oversampling template in both time and frequency domains to improve signal resolution and anti-distortion performance significantly (Selesnick, 2006). HDWT was implemented by three channel filters as described previously (Han et al., 2017b; Selesnick, 2006), where H_0 , H_1 and H_2 represent low-pass, band-pass and high-pass filters, respectively. This arrangement generates an expansive wavelet transform that possesses the approximately shift-invariant property, making HDWT robust against the distortion of Raman spectra.

After HDWT calculation, the CARSS removed uninformative HDWT coefficients. However, routine CARSS tends to generate a semi-random result that varied from run to run, which may not correlate well with the key ingredients in the yoghurt samples. To overcome this disadvantage of CARSS, a Monte Carlo strategy was performed to assign 60% training samples and 40% validation samples for multiple resampling of CARSS. The procedure was repeated 1000 times, generating a MCCARSS matrix with 1000 different sets of selected variables. The importance rank of each HDWT variable was determined by its frequency presented in the MCCARSS matrix, and then the optimal variable subset was determined by the principle of minimum root mean square error of cross-validation (RMSECV).

With the combination of the HDWT and MCCARSS, the features of key ingredients in yoghurt samples were digitally labelled for further calibration. In this work, the HDWT codes were written in Matlab 2016a based on the Selesnick (2006) methods. The program of partial least squares (PLS) and CARSS used an online library (Li et al., 2009), and MCCARSS was modified from CARSS in Matlab 2016a.

2.4. Reference method measurement

Determination of protein, fat, sucrose and total solids was performed before multivariate calibration, following the Peoples' Republic of China national standard GB5009.5–2016 for protein content (PRC, 2016), GB5413.3–2010 for fat content (PRC, 2010a), GB5413.5–2010 for sucrose content (PRC, 2010b) and GB5413.39–2010 for total solids (PRC, 2010c), respectively.

3. Results and discussion

3.1. Raman spectra of yoghurt samples

It is of great interest to investigate the Raman signals of yoghurt samples contained in the pipeline. Fig. 2 shows Raman spectra of yoghurt samples and blank samples (empty pipe) obtained from the pipeline, which allows a straightforward investigation of Raman signals of yoghurt samples.

As shown in Fig. 2, it is clear that the Teflon window generates strong Raman characteristic peaks ($287\text{--}294\text{ cm}^{-1}$, $382\text{--}386\text{ cm}^{-1}$, $432\text{--}437\text{ cm}^{-1}$, $520\text{--}530\text{ cm}^{-1}$, 730 cm^{-1} , 1217 cm^{-1} , $1292\text{--}1298\text{ cm}^{-1}$, $1375\text{--}1378\text{ cm}^{-1}$), and the spectral interference of the Teflon window increases when the yoghurt samples were injected. The reason is that the yoghurt samples are highly scattered systems, which greatly enhances the back scattered Raman signals. As a result, the spectral bands of yoghurt samples are overshadowed by the strong signals of Teflon window. Moreover, the matrix interference of yoghurt samples usually overlaps the spectral bands of key ingredients, thus greatly degrading the performance of on-line Raman spectroscopy. This creates a demand to develop a sophisticated chemometrics method for assigning Raman spectral bands to the components of interest.

3.2. Determination of HDWT parameters

HDWT represents a novel strategy for improving spectral resolution, and possesses the unique advantage of splitting spectral signals into localised time (wavelength position) and frequency domains (peak width resolution). In HDWT, there are four wavelet filters available for signal processing (Selesnick, 2006). Theoretically, a higher vanishing moment of the wavelet filter will generate higher spectral resolution, resulting in a more efficient suppression of background interference. In this regard, we utilised the 'bi4' wavelet filter with 4 vanishing moments for processing, since the 'bi4' wavelet filter possesses the highest vanishing moments in the current HDWT filter bank. As for the decomposition scale, we evaluated the relationship between scale parameter and measured RMSECV. According to the minimum RMSECV criterion, the decomposition scale was set as 6.

HDWT oversamples the Raman spectra in both of time and frequency domains by a factor of two, which is capable of

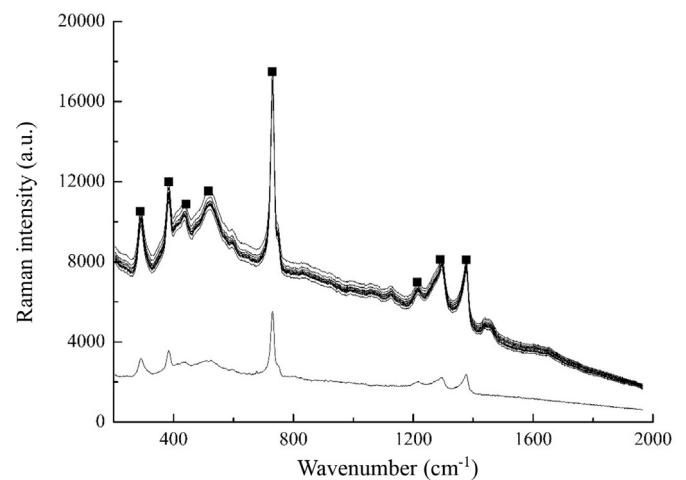


Fig. 2. Raman spectra obtained from the on-line monitoring pipeline, 10 samples of yoghurt samples (top line) and blank signals (bottom line); solid squares indicate peaks of Teflon.

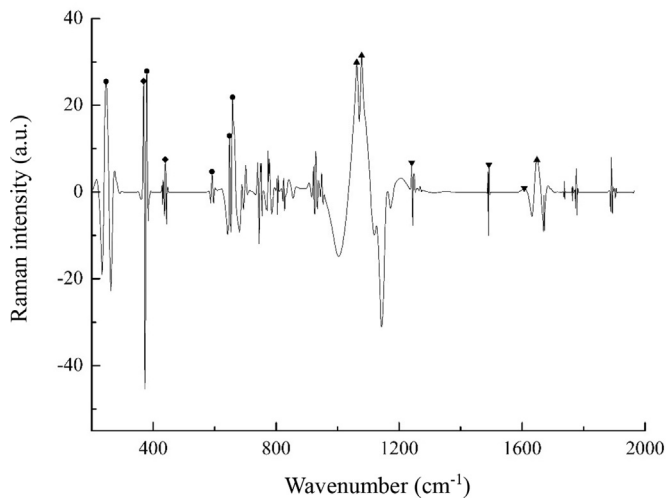


Fig. 3. Reconstructed Raman spectra obtained with the DLRS for prediction of total solids; peak identities are indicated as: ●, sucrose; ◆, lactose; ▲, fat; ▼, protein.

improving spectral resolution by resampling Raman signals at much higher rates. As a result, the original 1024 Raman spectral variables were expanded into 3040 variables, making an expandability rate nearly to be 3. It is thus expected that plenty of redundant variables will be introduced in the HDWT coefficients,

Table 1
Prediction result of key ingredients in yoghurt samples.

Component	PLS factors	R	RMSEP	R/A (%)
PLS				
Protein	7	0.294	0.059	2.02%
Fat	7	0.617	0.093	2.95%
Sucrose	11	0.680	0.162	2.24%
Total solids	7	0.788	0.171	0.96%
DLRS				
Protein	3	0.919	0.029	1.00%
Fat	3	0.923	0.046	1.47%
Sucrose	3	0.933	0.076	1.05%
Total solids	4	0.875	0.153	0.87%

Table 2
The DLRS prediction results for protein, fat, sucrose, and total solids as well as measured values.

Sample	Protein value (%)		Fat value (%)		Sucrose value (%)		Total solids value (%)	
	Measured	Predicted	Measured	Predicted	Measured	Predicted	Measured	Predicted
1	2.91	2.89	3.38	3.37	7.48	7.45	17.78	17.93
2	2.99	2.96	3.28	3.29	7.15	7.20	17.49	17.57
3	3.07	2.99	3.05	3.05	7.50	7.50	18.03	17.91
4	2.91	2.88	3.18	3.15	7.18	7.23	17.62	17.56
5	2.86	2.89	3.10	3.10	7.25	7.16	17.21	17.37
6	2.89	2.88	2.99	3.05	6.77	6.80	17.31	17.21
7	2.99	2.93	3.29	3.21	7.44	7.42	18.15	18.07
8	2.92	2.90	3.02	3.05	7.66	7.50	17.98	17.84
9	2.96	2.96	3.29	3.24	7.15	7.08	18.29	18.42
10	2.93	2.94	3.25	3.20	7.14	7.21	17.67	17.73
11	2.89	2.89	3.06	3.12	7.26	7.28	17.32	17.18
12	2.91	2.92	2.97	2.99	7.04	7.19	17.37	17.49
13	2.77	2.82	3.15	3.11	7.30	7.36	17.82	18.05
14	2.91	2.91	3.11	3.07	7.12	7.26	17.44	17.59
15	2.91	2.93	3.15	3.20	7.03	7.11	17.50	17.69
16	2.93	2.95	3.11	3.12	7.04	7.15	17.59	17.48
17	3.08	3.04	2.91	3.00	7.47	7.38	17.70	17.76
18	2.93	2.91	3.12	3.21	6.80	6.74	17.41	17.62
19	2.91	2.90	3.07	3.13	7.41	7.34	17.82	17.90
20	2.90	2.91	3.28	3.26	7.29	7.31	18.06	18.39
21	2.92	2.92	3.09	3.04	7.15	7.16	17.77	17.52
22	2.93	2.92	3.24	3.22	7.11	7.14	17.66	17.78
23	2.92	2.92	3.21	3.19	7.30	7.28	17.73	17.58
24	2.93	2.90	3.21	3.19	7.18	7.12	17.64	17.77

requiring a sophisticated feature selection strategy for isolating irrelevant HDWT coefficients.

3.3. Variables selection through MCCARSS

MCCARSS aims to eliminate uninformative HDWT coefficients. With the combination of the HDWT and MCCARSS, informative variables related to 4 key ingredients in yoghurt samples are extracted and transferred to a final DLRS model.

It is of great interest to investigate the DLRS reconstructed spectral information, which presents a straightforward tool for investigating the results of feature selection. As for the 4 key ingredients mentioned above, the total solids in homogenised yoghurt samples includes the information of protein, fat, sucrose, lactose, inorganic content and other components as well. It is thus expected that the DLRS reconstructed spectra of the total solids reveal the feasibility of the DLRS strategy straightforwardly.

As shown in Fig. 3, the reconstructed Raman spectrum of the total solids clearly shows the characteristic peaks of the protein (1240 cm^{-1} , 1492 cm^{-1} , 1610 cm^{-1}) (Baena & Lendl, 2004; Gelder, Gussem, Vandenabeele, & Moens, 2007), fat (1062 cm^{-1} , 1079 cm^{-1} , 1650 cm^{-1}) (Czamara et al., 2015), sucrose (247 cm^{-1} , 378 cm^{-1} , 648 cm^{-1} , 659 cm^{-1}) (Branca, Magazu, Maisano, Bennington, & Fak, 2003) and lactose (369 cm^{-1} , 440 cm^{-1}) (Veij, Vandenabeele, Beer, Remon, & Moens, 2010). In Fig. 3, the Raman features selected by DLRS fit well with chemical groups, e.g., the stretch and bending vibrations associated with C–H, C–O–C, N–H, O–H and O–O bonds, providing evidence that DLRS extracts the informative spectral features in the presence of matrix interference.

3.4. Prediction results

Table 1 summarises the DLRS prediction results for the 4 key ingredients in yoghurt samples including protein, fat, sucrose and total solids, together with the PLS prediction results. It was found that the PLS models are acceptable, illustrating that the on-line Raman system has potential as a gauge for monitoring the 4 key ingredients in yoghurt samples. However, these plain PLS models do not achieve a satisfactory prediction accuracy, and the PLS

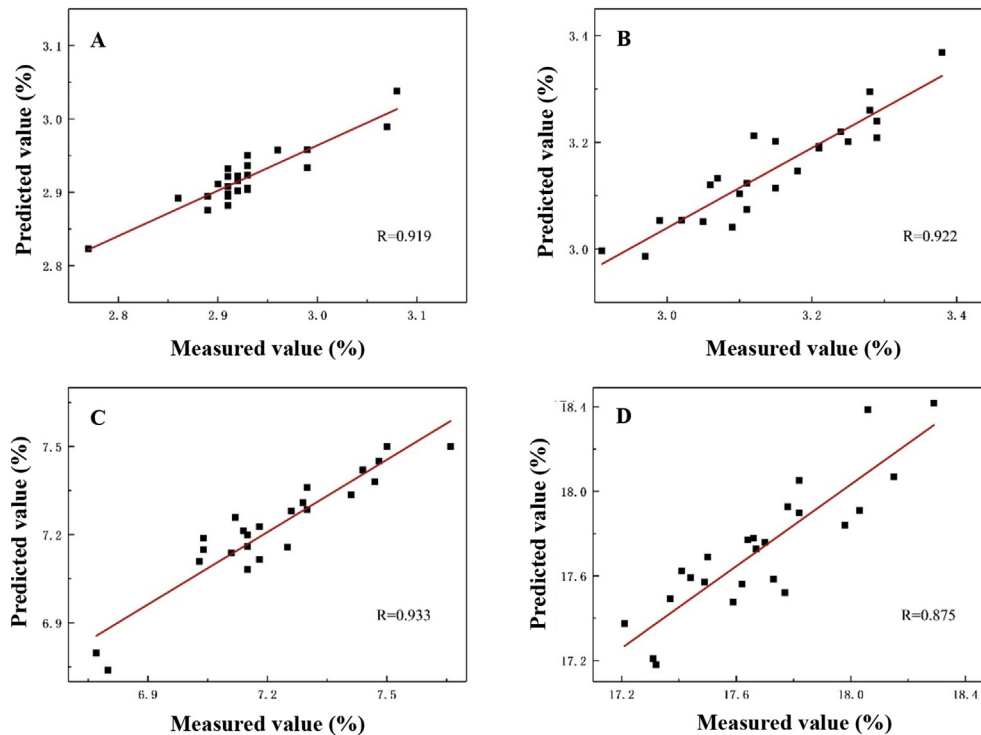


Fig. 4. The DLRS prediction results for (A) protein, (B) fat, (C) sucrose, (D) total solids.

factors are abnormally high, which greatly increases the risk of overfitting. The reason is that the spectral bands of the 4 key ingredients are often overlapped with the matrix of yoghurt samples and Teflon windows, and the isolation of these important features before calibration is critical to promote the calibration performance.

To improve calibration performance of the PLS models, the DLRS is proposed to select the most important variables for modelling. Table 1 summarises the prediction results obtained with DLRS. The PLS factors required by the DLRS are only 3, ensuring that the constructed DLRS models are more robust and reliable than those of PLS models. Results in Table 1 also illustrate that DLRS improves the calibration performance of PLS models significantly, no matter correlation coefficients or prediction accuracy. To validate the reliability of the DLRS prediction results, a two-sample T-test with 93% confidence was adopted (Cohen, 1988). The results indicate that there is no significant difference between predicted and true values.

It is also of great interest to investigate whether prediction accuracy of DLRS satisfies the mandatory requirement. According to the document 'A Food Labeling Guide – Guidance for Industry' suggested by the Food and Drug Administration of USA (FDA, 2013), the relative error of the prediction results should be mandatorily controlled within 20%. As shown in Table 1, it is clear that the prediction accuracy satisfies the mandatory requirement well. Table 2 and Fig. 4 show the measured values versus the prediction results obtained with DLRS. It straightforwardly reveals that DLRS provides a promising tool for on-line monitoring of 4 key ingredients in yoghurt samples. What should be stressed is that the prediction accuracy will be naturally worse when the concentration ranges of the 4 nutrients are enlarged.

4. Conclusions

This study presented a DLRS system for on-line monitoring of the 4 key ingredients in homogenised yoghurt samples before

fermentation, which increases the quality control level of yoghurt products. DLRS performs the MCCARSS in the HDWT domain instead of the raw Raman spectral domain, suppressing the matrix effect on calibration model efficiently. With the combination of on-line Raman system, DLRS is capable of on-line monitoring of the 4 key ingredients in yoghurt samples. The DLRS system is validated by means of systematic analysis of the 72 practical samples, which yields the challenges representative of those encountered in a common dairy analysis. The satisfactory results illustrate that this method extracts the spectral features of the 4 key ingredients in yoghurt samples accurately, making it capable of monitoring yoghurt samples automatically and continuously without sample preparation. The DLRS system can be also applied to other kinds of dairy products as well.

Acknowledgements

This work is supported by the National Key R&D Program of China (2018YFF01011700), National Natural Science Foundation of China (61378048, 21305101), 100 Talents Plan of Hebei Province (E2014100007), Talents for Technology-based Enterprises of Hebei Province (169A76348H).

References

- Baena, J. R., & Lendl, B. (2004). Raman spectroscopy in chemical bioanalysis. *Current Opinion in Chemical Biology*, 8, 534–539.
- Branca, C., Magazu, S., Maisano, G., Bennington, S. M., & Fak, B. (2003). Vibrational studies on disaccharide/H₂O systems by inelastic neutron scattering, Raman, and IR Spectroscopy. *Journal of Physical Chemistry B*, 107, 1444–1451.
- Brennan, D., Alderman, J., Sattler, L., O'Connor, B., & O'Mathuna, C. (2003). Issues in development of NIR micro spectrometer system for on-line process monitoring of milk product. *Measurement*, 33, 67–74.
- Castiglioni, S., Bagnati, R., Calamari, D., Fanelli, R., & Zuccato, E. (2005). A multiresidue analytical method using solid-phase extraction and high-pressure liquid chromatography tandem mass spectrometry to measure pharmaceuticals of different therapeutic classes in urban wastewaters. *Journal of Chromatography A*, 1092, 206–215.
- Chen, D., Cai, W., & Shao, X. (2007). Representative subset selection in modified iterative predictor weighting (mIPW) — PLS models for parsimonious

- multivariate calibration. *Chemometrics and Intelligent Laboratory Systems*, 87, 312–318.
- Cohen, J. (1988). The t test for means. Statistical power analysis for the behavioral sciences. *Technometrics*, 31, 499–500.
- Czamara, K., Majzner, K., Pacia, M. Z., Kochan, K., Kaczor, A., & Baranska, M. (2015). Raman spectroscopy of lipids: A review. *Journal of Raman Spectroscopy*, 46, 4–20.
- Doganis, P., & Sarimveis, H. (2007). Optimal scheduling in a yoghurt production line based on mixed integer linear programming. *Journal of Food Engineering*, 80, 445–453.
- FDA. (2013). *Labeling and nutrition - guidance for industry: A food labeling guide*. Available from: <https://www.fda.gov/food/guidanceregulation/guidancedocument/entireinformation/labelingnutrition/ucm2006828.htm>.
- Feudale, R. N., Liu, Y., Woody, N. A., Tan, H., & Brown, S. D. (2005). Wavelet orthogonal signal correction. *Journal of Chemometrics*, 19, 55–63.
- Fitzgerald, N., McGrath, M. J., O'Connor, J. F., & Phelan, N. (1998). Integration of on-line quality control into the process control environment for cheese manufacturing. *Food Control*, 9, 369–377.
- Gelder, J. D., Gussem, K. D., Vandenabeele, P., & Moens, L. (2007). Reference database of Raman spectra of biological molecules. *Journal of Raman Spectroscopy*, 38, 1133–1147.
- Gomez-Carracedo, M. P., Andrade, J. M., Rutledge, D. N., & Faber, N. M. (2007). Selecting the optimum number of partial least squares components for the calibration of attenuated total reflectance-mid-infrared spectra of undesigned kerosene samples. *Analytica Chimica Acta*, 585, 253–265.
- Han, X., Huang, Z. X., Chen, X. D., Li, Q. F., Xu, K. X., & Chen, D. (2017a). On-line multi-component analysis of gases for mud logging industry using data driven Raman spectroscopy. *Fuel*, 207, 146–153.
- Han, X., Huang, Z. X., Wang, S. F., Chen, X. D., Li, Q. F., Xu, K. X., et al. (2017b). New insights to improve resolution and reliability of Raman spectral analysis using higher-density multiscale regression. *Chemometrics and Intelligent Laboratory Systems*, 169, 110–115.
- Han, X., Tan, Z., Huang, Z. X., Chen, X. D., Gong, Y., Li, Q. F., et al. (2017c). Non-destructive detection of triclosan in antibacterial hand soaps using digitally labelled Raman spectroscopy. *Analytical Methods*, 9, 3720–3726.
- Ipsen, R. (2017). Microparticulated whey proteins for improving dairy product texture. *International Dairy Journal*, 67, 73–79.
- Jones, J. B., Jr. (1991). *Kjeldahl method for nitrogen determination*. Athens, GA, USA: Micro-Macro Publishing, Inc.
- Karoui, R., Mazerolles, G., & Dufour, E. (2003). Spectroscopic techniques coupled with chemometric tools for structure and texture determinations in dairy products. *International Dairy Journal*, 13, 607–620.
- Li, H., Liang, Y., Xu, Q., & Cao, D. (2009). Key wavelengths screening using competitive adaptive reweighted sampling method for multivariate calibration. *Analytica Chimica Acta*, 648, 77–84.
- Liu, Y., & Brown, S. D. (2004). Wavelet multiscale regression from the perspective of data fusion: New conceptual approaches. *Analytical and Bioanalytical Chemistry*, 380, 445.
- Lopez-Garcia, E., Leon-Munoz, L., Guallar-Castillon, P., & Rodriguez-Artalejo, F. (2015). Habitual yogurt consumption and health-related quality of life: A prospective cohort study. *Journal of the Academy of Nutrition and Dietetics*, 115, 31–39.
- Luo, Q., Li, X., Gu, Y., Tang, Y., Tan, Z., & Chen, D. (2016). A method based on coffee-ring deposition confocal Raman spectroscopy of analysis of melamine in milk. *Optics in Health Care and Biomedical Optics VII*, 10024. Article 1002426.
- Nieuwoudt, M. K., Holroyd, S. E., McGovern, C. M., Simpson, M. C., & Williams, D. E. (2016). Rapid, sensitive, and reproducible screening of liquid milk for adulterants using a portable Raman spectrometer and a simple, optimized sample well. *Journal of Dairy Science*, 99, 7821–7831.
- Pereira, R. B., Singh, H., Munro, P. A., & Luckman, M. S. (2003). Sensory and instrumental textural characteristics of acid milk gels. *International Dairy Journal*, 13, 655–667.
- PRC. (2010a). *National food safety standard. Determination of fat in foods for infants and young children, milk and milk products*, 5413.3–2010. Beijing, Peoples' Republic of China: Ministry of Health.
- PRC. (2010b). *National food safety standard. Determination of lactose and sucrose in foods for infants and young children, milk and milk products*, 5413.5-2010. Beijing, Peoples' Republic of China: Ministry of Health.
- PRC. (2010c). *National food safety standard. Determination of nonfat total milk solids in milk and milk products*, 5413.39-2010. Beijing, Peoples' Republic of China: Ministry of Health.
- PRC. (2016). *National food safety standard. Determination of protein*, 5009.5-2016. Beijing, Peoples' Republic of China: Ministry of Health.
- Rodriguez, R., Vargas, S., Estevez, M., Quintanilla, F., Trejo-Lopez, A., & Hernandez-Martinez, A. R. (2013). Use of Raman spectroscopy to determine the kinetics of chemical transformation in yoghurt production. *Vibrational Spectroscopy*, 68, 133–140.
- Roupas, P. (2008). Predictive modelling of dairy manufacturing processes. *International Dairy Journal*, 18, 741–753.
- Selesnick, I. W. (2006). A higher density discrete wavelet transform. *IEEE Transactions on Signal Processing*, 54, 3039–3048.
- Singh, G., & Muthukumarappan, K. (2008). Influence of calcium fortification on sensory, physical and rheological characteristics of fruit yoghurt. *LWT Food Science and Technology*, 41, 1145–1152.
- Tan, Z., Lou, T. T., Huang, Z. X., Zong, J., Xu, K. X., Li, Q. F., et al. (2017). Single-drop Raman imaging exposes the trace contaminants in milk. *Journal of Agricultural and Food Chemistry*, 65, 6274–6281.
- Torres, I. C., Janhøj, T., Mikkelsen, B.Ø., & Ipsen, R. (2011). Effect of microparticulated whey protein with varying content of denatured protein on the rheological and sensory characteristics of low-fat yoghurt. *International Dairy Journal*, 21, 645–655.
- Tsarouhas, P. H., & Arvanitoyannis, I. S. (2014). Yoghurt production line: Reliability analysis. *Production and Manufacturing Research*, 2, 11–23.
- Vejj, M. D., Vandenabeele, P., Beer, T. D., Remon, J. P., & Moens, L. (2010). Reference database of Raman spectra of pharmaceutical excipients. *Journal of Raman Spectroscopy*, 40, 297–307.
- Wang, X., Esquerre, C., Downey, G., Henihan, L., O'Callaghan, D., & O'Donnell, C. (2017). Feasibility of discriminating dried dairy ingredients and preheat treatments using mid-infrared and Raman spectroscopy. *Food Analytical Methods*, 11, 1380–1389.
- Williams, E. B., Hooper, B., Spiro, A., & Stanner, S. (2015). The contribution of yoghurt to nutrient intakes across the life course. *Nutrition Bulletin*, 40, 9–32.
- Wojciechowski, K. L., Melilli, C., & Barbano, D. M. (2016). A proficiency test system to improve performance of milk analysis methods and produce reference values for component calibration samples for infrared milk analysis. *Journal of Dairy Science*, 99, 6808–6827.
- Woody, N. A., & Brown, S. D. (2010). Selecting wavelet transform scales for multivariate classification. *Journal of Chemometrics*, 21, 357–363.